

Article

Experimental Study on Reducing CO₂–Oil Minimum Miscibility Pressure with Hydrocarbon Agents

Junrong Liu ^{1,2,*} , Lu Sun ³, Zunzhao Li ⁴ and Xingru Wu ⁵

¹ Key Laboratory of Unconventional Oil & Gas Development (China University of Petroleum (East China)), Ministry of Education, Qingdao 266580, China

² School of Petroleum Engineering, China University of Petroleum (East China), Qingdao 266580, China

³ Dongming Petroleum Distribution Company, Shandong Dongming Petrochemical Group Co., Ltd., Heze 274000, China; sunlu@dmpec.com.cn

⁴ Dalian Petrochemical Research Institute, Dalian 116045, China; lizunzhao.fshy@sinopec.com

⁵ Mewbourne School of Petroleum & Geological, The University of Oklahoma, 100 E. Body St. SEC1362, Norman, OK 73019, USA; xingru.wu@ou.edu

* Correspondence: junrliu@upc.edu.cn; Tel.: +86-186-0546-9979

Received: 8 April 2019; Accepted: 21 May 2019; Published: 23 May 2019



Abstract: CO₂ flooding is an important method for improving oil recovery for reservoirs with low permeability. Even though CO₂ could be miscible with oil in regions nearby injection wells, the miscibility could be lost in deep reservoirs because of low pressure and the dispersion effect. Reducing the CO₂–oil miscibility pressure can enlarge the miscible zone, particularly when the reservoir pressure is less than the needed minimum miscible pressure (MMP). Furthermore, adding intermediate hydrocarbons in the CO₂–oil system can also lower the interfacial tension (IFT). In this study, we used dead crude oil from the H Block in the X oilfield to study the IFT and the MMP changes with different hydrocarbon agents. The hydrocarbon agents, including alkanes, alcohols, oil-soluble surfactants, and petroleum ethers, were mixed with the crude oil samples from the H Block, and their performances on reducing CO₂–oil IFT and CO₂–oil MMP were determined. Experimental results show that the CO₂–oil MMP could be reduced by 6.19 MPa or 12.17% with petroleum ether in the boiling range of 30–60 °C. The effects of mass concentration of hydrocarbon agents on CO₂–oil IFT and crude oil viscosity indicate that the petroleum ether in the boiling range of 30–60 °C with a mass concentration of 0.5% would be the best hydrocarbon agent for implementing CO₂ miscible flooding in the H Block.

Keywords: CO₂ miscible flooding; interfacial tension; minimum miscibility pressure; hydrocarbon agent

1. Introduction

CO₂ is a greenhouse gas and an effective oil displacement agent. Injecting carbon dioxide into an oil reservoir to enhance oil recovery and realize carbon dioxide geological storage has profound impacts on reducing carbon emission and maintaining sustainable development of an oil field. Supercritical CO₂ flooding is a proven tertiary oil recovery technology with an increasingly positive track record in the United States and other regions for the past 40 years [1]. Gas injection, mainly CO₂ flooding, produces approximately 60% of domestic tertiary oil recovery in the US, and thermal enhanced oil recovery (EOR) methods produce another 40%, while all chemical methods combined produce less than 1% of domestic tertiary oil [2]. Many properties of CO₂ make it an ideal agent for EOR purposes. At reservoir conditions (reservoir pressure greater than 1200 psia and temperature less than 250 °F), CO₂ can be miscible with a wide range of crude oils through a multi-contact miscibility process [3]. Even for

reservoirs with temperatures below 120 °F (49 °C), some liquid/liquid and liquid/liquid/vapor equilibria could occur during EOR [4]. In the Permian Basin alone, more than 1.6 BCF/D of naturally-sourced CO₂ is injected into oil fields to produce 170 MSTB/D of crude oil [5]. Furthermore, for reservoirs with low permeability and/or heavy oils, CO₂ miscible flooding can also be an effective EOR method. For example, the technical limit for CO₂ miscible flooding is about 1.1 billion tons in China alone [6].

The CO₂ injected into an oil-bearing reservoir will swell oil and reduce oil–water IFT and oil viscosity after dissolved in crude oil. The synergetic mechanisms significantly increase oil recovery [7]. Additionally, CO₂ flooding can supplement reservoir energy by effectively injecting supercritical CO₂ into a reservoir with low permeability. Therefore, it is very suitable for improving oil recovery in low permeability reservoirs. Additionally, CO₂ flooding has two advantages: (1) CO₂ can achieve miscibility at a lower pressure than methane; (2) injection of CO₂ can help carbon dioxide sequestration to a certain extent by reducing greenhouse gas emissions [8,9]. In addition to continuous CO₂ flooding, CO₂ huff-n-puff is also considered as a preferred approach for ultra-low permeability reservoirs, or it can be used as a precursor technique for CO₂ flooding [10–13].

In the late 1950s, the earliest CO₂ miscible flooding project had been implemented in the Permian Basin. Field test results showed that CO₂ flooding was an effective EOR method [14]. TPAO (Turkish Petroleum Corporation), JNOC (Japan National Oil Corporation), and JEORA (Japan EOR Research Association) conducted a CO₂ immiscible flooding field test in the Ikiztepe oilfield with a 200 m/200 m inverted five-spot well pattern. The test results proved that CO₂ immiscible flooding was a promising method for improving oil recovery in low permeability reservoirs [15]. In 1972, the world's first commercial CO₂-EOR project with nine well groups was implemented at the SACROC (Scurry Area Canyon Reef Operators Committee) block of the Kelly-Snyder oilfield in Texas, US, with an initial average production increase of more than three times per well [16]. In 2014, the CO₂ flooding well groups in this block increased to 503, and the annual EOR production was up to 138×10^4 t. CO₂ miscible flooding projects in the US were mainly implemented in low-porosity and low-permeability reservoirs. The average porosity and permeability were 13.23% and $38.1 \times 10^{-3} \mu\text{m}^2$. The minimum porosity and permeability were 3.00% and $1.5 \times 10^{-3} \mu\text{m}^2$. According to the statistical data of the 2014 worldwide EOR project, a total of 128 CO₂ miscible flooding and nine CO₂ immiscible flooding projects were conducted in the US, and 81.25% of CO₂ miscible flooding projects were successful. Among these projects, there were 52 reservoirs with permeability lower than $10 \times 10^{-3} \mu\text{m}^2$, and the average production per well was 2.43 t/d [17–22]. CO₂ slug miscible flooding technology also has been successfully applied in the Olikhov oilfield, where the oil recovery reached up to 94%~99% with larger CO₂ slugs [19]. While the injection of CO₂ has great potential for increasing oil production, this potential is limited by many site conditions and operational constraints, including limited economical CO₂ sources, CO₂-associated corrosion of infrastructure, lack of adequate infrastructure, and premature breakthrough of injected CO₂. Sourcing CO₂ for EOR is a location specific and costly process. Anthropogenic CO₂, such as that produced by power plants, needs to be captured, compressed, and routed to the injection site, which makes the CO₂ a very expensive commodity. Additionally, a CO₂ recycle plant needs to be constructed for conventional CO₂ flooding. These factors make miscible CO₂ limited to particular locations and fields. For example, there is still no commercial application of CO₂-EOR in the North Sea [23–25]. However, the combination of EOR and CCS (carbon capture and storage) is considered as a more profitable situation in the North Sea [25,26].

CO₂ flooding was widely tested and applied in China, and some prominent results for EOR were realized. In the X oilfield, a CO₂ flooding project was conducted in an abandoned oil reservoir with water-alternating-CO₂ technology. After injecting 0.65 PV of water and 0.29 PV of CO₂ in the Pu 1-1 well group, the cumulative oil production increased 5753 t, and the incremental recovery factor of OOIP (Original Oil in Place) was up to 6.5%. The density and the viscosity of the produced oil decreased from 0.864 g/cm³ to 0.835 g/cm³ and from 24.66 mPa·s to 7.99 mPa·s, respectively. Additionally, the intermediate hydrocarbon components increased, and heavy hydrocarbon components decreased. The project showed that the injected CO₂ displaced unswept regions from water flooding, and CO₂

achieved miscible flooding in the formation [27]. In the Pubei oilfield, both flowing bottomhole pressure and formation pressure were higher than the CO₂–oil minimum miscible pressure (MMP) in CO₂ flooding; fluid viscosity decreased from 0.67 mPa·s to 0.20 mPa·s, bubble point pressure increased from 29.44 MPa to 32.86 MPa, and intermediate hydrocarbon components in produced oil increased from 23.79% to 25.12% [28]. Other field tests in the Daqing and the Shengli oilfields stated that CO₂ miscible flooding could improve oil recovery by 4.7%–17.2%. Most of the field tests disclosed that CO₂ miscible flooding played a dominant role in improving oil recovery. However, CO₂ miscible flooding cannot be fully implemented in some reservoirs, particularly in highly depleted reservoirs. For these reservoirs, even if the miscibility is achieved in the near wellbore region due to high injection pressure, the miscibility may break in the deep reservoir if the pore pressure is less than the needed miscibility pressure [29,30].

For reservoirs that cannot realize CO₂ miscible flooding under their own reservoir pressures, there are two ways to realize miscible flooding. One way is to increase formation pressure by injecting water or gas to achieve the minimum miscibility pressure. Another way is to change the properties of oil and CO₂ and thus change their interactions to achieve miscible flooding. Based on the analysis of Cooper Basin (located in central Australia) reservoir fluid, Bon et al. proposed to reduce the MMP by adding a small pentanes-plus fraction into CO₂ to significantly reduce the MMP from 23.7 MPa to 19.8 MPa in their study [31]. Liu et al. found that the MMP of CO₂–oil would be significantly reduced after adding miscible solvent into crude oil. The miscible solvent can be some light components, such as propane or butane [32].

The H Block in the X oilfield has low permeability, high temperature, and a salinity reservoir. Conventional chemical flooding could not achieve a desirable result. CO₂ EOR was used for this Block. The reservoir depth in the H Block ranges from 1880 m to 2550 m, and its reservoir pressure coefficient is around 1.0. The reservoir pressure is far lower than CO₂–oil MMP. Therefore, reducing CO₂–oil MMP is an important way to develop this reservoir efficiently. In this paper, the effect of hydrocarbon agents on CO₂–oil MMP was studied firstly by laboratory experiments. Then, the mechanisms of reducing CO₂–oil MMP by hydrocarbon agents were discussed. Four types of hydrocarbon agents (including alkanes, alcohols, oil soluble, and petroleum ether) were used to evaluate their performances on reducing CO₂–oil MMP, and a suitable hydrocarbon agent and its concentration were successfully screened. Finally, the injection capacity of the hydrocarbon agent was measured.

2. Mechanism of Reducing CO₂–Oil MMP with a Hydrocarbon Agent

In different reservoirs, the factors affecting CO₂ flooding miscibility pressure are different due to different reservoir conditions and oil properties. In regard to the H Block in the X oilfield, the main factors affecting its MMP are reservoir temperature, injected gas composition, oil properties, CO₂ extraction capacity, and CO₂ solubility in oil [33]. Decreasing the reservoir temperature and changing the injected gas composition are two methods to achieve CO₂ miscible flooding. However, it is difficult to decrease reservoir temperature, and gas source is a limiting factor affecting injected gas composition. Therefore, it is necessary to find a suitable hydrocarbon agent to decrease CO₂–oil IFT and further reduce MMP.

2.1. Experiment on Reducing CO₂–Oil Interfacial Tension with Petroleum Ether

In the process of CO₂ flooding, the IFT between the displacing CO₂ phase and the in situ oil phase usually becomes less and less with the increase of CO₂ concentration in the oil phase. Once a miscible state is achieved, the IFT should be zero. The CO₂–oil IFT was measured with interfacial tensiometer after adding petroleum ether in order to study the effect of reducing CO₂–oil IFT by the hydrocarbon agent.

2.1.1. Sample Preparation

The crude oil was sampled from a wellhead at the H block in the X oilfield and dehydrated for laboratory experiments. The dead oil density was 0.8512 g/cm³, and the oil viscosity was 9.8 mPa·s at

70 °C. The detailed dead oil components and the compositions are listed in Table 1. The CO₂ purity used in the experiments was 99.9%. In the tested sample, the light ends (C1–C4) did not exist in the crude oil, which may have led to a different MMP when compared with live crude oil samples. Some empirical correlations for MMP predication indicated that C1 and C7+ (heavy content) compositions had a positive correlation with the MMP, while C2–C6 compositions had a negative correlation [34–36]. However, the correlations often only fit a specific reservoir.

Table 1. Composition of dead crude oil components used in this study.

Components	C1–C4	C5–C8	C9–C12	C13–C18	C19–C22	C23–C27	C28+
Mole fraction (%)	0	14.972	10.067	28.737	13.778	15.918	16.529

2.1.2. Experimental Instrument

The methods of measuring CO₂–oil MMP in the laboratory included the bubble rising method [37,38], the IFT method [39,40], the slim tube method [41], the magnetic resonance imaging method [32], the acoustically monitored separator method [42], and so on. Among these, the slim tube method is the most reliable and classical experimental method, but it is time-consuming, has a higher cost, and lacks uniform criteria [43]. The bubble rising method requires a shorter time and has a reliable result. However, the observed bubble appearance is affected by the lower light transmittance when the oil color is dark and thus lacks quantitative information [38]. The magnetic resonance imaging method uses image intensity to deduce the minimum pressure when the proton densities of the hydrocarbon in the liquid and the gas rich phases are equal. It is costly due to the expensive equipment facility and the high demand for electric current supply [32]. The acoustically monitored separator method provides real volume distribution of two fluids and their interface without encroachment into the system. It also requires a relatively low capital and avoids radiation exposure. However, its measurement accuracy is adversely affected by the phenomena of emulsion during mixing two fluids [42]. The IFT method is based on the concept that IFT between a crude oil and CO₂ becomes zero when they are miscible. The CO₂–oil MMP can be estimated by extrapolating the experimental data to intersect with the pressure axis where the IFT is equal to zero. It is a simple and indirect method in which the measuring time is shorter and the consumed oil is less. This method is based on theory described in literature [39,40].

In this study, a high temperature and high pressure interfacial tensiometer (Figure 1) was used to determine CO₂–oil MMP from measuring IFT. A needle located in the central part of the high temperature and high pressure autoclave was used to form a fluid pendant droplet. When the reactor was raised to a certain pressure and temperature, liquid was slowly squeezed out of the needle using a hand pump to form a pendant droplet. A high speed camera was used to record the shape changing process of the droplet, and pictures were analyzed with shape analysis software [44]. Using the captured shape data, we calculated the IFT according to the surface selection method proposed by Andreas et al. [45].

The exact MMP at the moment of zero IFT may not have been accurately determined by the IFT method. The traditional method is to linearly extrapolate the measured data to obtain the pressure at which IFT is zero [46].

The experiment devices included a high pressure and high temperature interfacial tensiometer, a CO₂ storage bottle, a CO₂ intermediate container, a crude oil intermediate container, a constant flow pump, needle valves, and so on. The schematic diagram of the IFT experimental apparatus is shown in Figure 2.



Figure 1. High pressure and high temperature interfacial tensiometer.

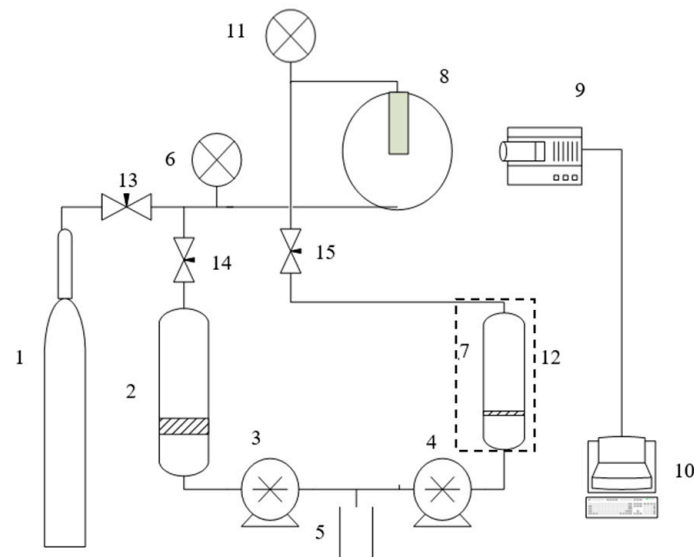


Figure 2. Schematic diagram of the interfacial tension (IFT) experimental apparatus. (1) CO₂ storage bottle, (2) CO₂ intermediate container, (3) constant flow pump, (4) manual pump, (5) water storage tank, (6) and (11) pressure gauge, (7) crude oil intermediate container, (8) high pressure and high temperature interfacial tensiometer, (9) camera, (10) computer, (12) insulated device, (13) and (14) gas needle valve, (15) oil needle valve.

2.1.3. Experimental Procedures

(1) Preparing samples. Pour 50 g of dehydrated crude oil into a cleaned sample bottle. Then, add 0.5% mass concentration of petroleum ether and shake them to mix evenly. Then, put the sample bottle in a water bath pot with a constant temperature of 70 °C and keep it over 12 hours to make petroleum ether and crude oil fully mixed. Finally, transfer the petroleum ether and crude oil mixture into the crude oil intermediate container.

(2) Clean the whole experiment system (including instrument, connected lines) with petroleum ether, and then purge the experiment system with hot air to remove the remaining petroleum ether in the connected lines.

(3) Vacuum the experiment system, inject pure CO₂, and discharge it to minimize the impact of air on the measurement.

(4) Close all needle valves and heat the autoclave to 109 °C. Open the CO₂ storage bottle, inject the CO₂ into the autoclave room, and keep the temperature constant. After the pressure between the autoclave room and CO₂ storage bottle achieve a balance, close gas needle valve 13 and open gas needle valve 14. The CO₂ intermediate container is used to further pressurize the autoclave room to 20 MPa. Then, close all gas needle valves.

(5) Pressurize the crude oil intermediate container to 7 to 20 MPa with manual pump 4. Open oil needle valve 15 and change the manual pump slowly. Observe the oil droplet formed at the needle end. When the oil droplet is about to fall off, ensure it remains in this state for 1 minute to stabilize it. Take photos with the camera system and calculate the IFT with the surface selection method.

(6) Close oil needle valve 15, open gas needle valve 14, start the constant flow pump to pressurize the autoclave room, and repeat Step 5 to obtain IFTs at pressures step-wisely. Increase pressure by 2 MPa in each step until reaching the final pressure of 40 MPa.

2.2. Experimental Results

When the mixture of petroleum ether and crude oil contacted with CO₂ under different pressures, the oil droplet formed at the needle end showed different shapes, as shown in Figure 3. With the increase of pressure, the oil droplet shape became thinner and longer and finally reached the miscible state. At this condition, the CO₂-oil IFT was zero, and the oil droplet could not be formed. When the pressure was in the range of 20-28 MPa, the oil droplet shape did not change significantly. When the pressure was in the range of 34-38 MPa, the oil droplet was pulled longer. As the pressure reached 46 MPa, the oil became a mist fluid rapidly [47]. Finally, it reached a miscible state. In the experiment, two distinct characteristics could be observed before the crude oil and the CO₂ reached the miscible state: (1) they were unable to form a complete fluid droplet (it was considered that the IFT was equal to zero at this time), and a relatively obvious wire drawing phenomenon occurred; (2) the light components in crude oil showed an obvious mist phenomena with diffusing to CO₂.

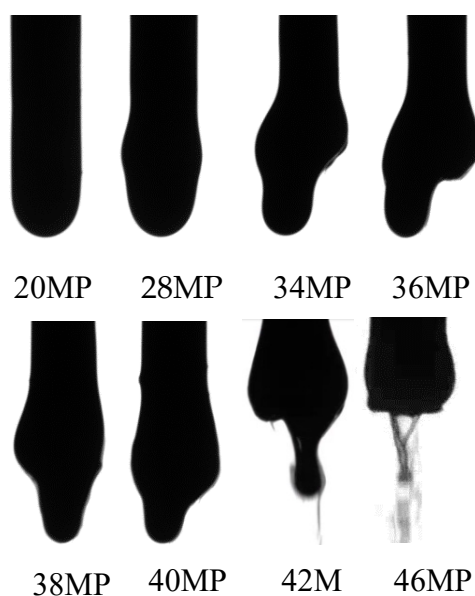


Figure 3. Droplet shapes under different pressures after adding petroleum ether in the crude oil.

The calculated CO₂-oil IFTs under different pressures are shown in Table 2. Although the MMP could have been determined by observing the corresponding pressure when the oil droplet could not be formed, the experimental process would have been longer, and the process control would have been difficult. Figure 4 shows that the IFT had a linear relation with pressure; therefore, the CO₂-oil MMP could be obtained with the linear extrapolation method. The calculated CO₂-oil MMPs for the original crude oil and the mixture of crude oil and petroleum ether were 50.86 MPa and 42.70 MPa,

respectively. The reduction of MMP was about 16.0% after adding petroleum ether into crude oil. This indicates that the CO₂–oil MMP could be effectively reduced by adding some hydrocarbon agents.

Table 2. Calculated CO₂–oil interfacial tensions under different pressures.

Pressure (MPa)	CO ₂ –Oil Interfacial Tension (mN/m)	
	with Petroleum Ether	without Petroleum Ether
20	3.55	4.18
22	3.26	3.82
24	2.77	3.45
26	2.49	3.06
28	2.09	2.88
30	1.72	2.56
32	1.39	2.45
34	1.16	2.06
36	0.95	2.02
38	0.80	1.65
40	0.71	1.56

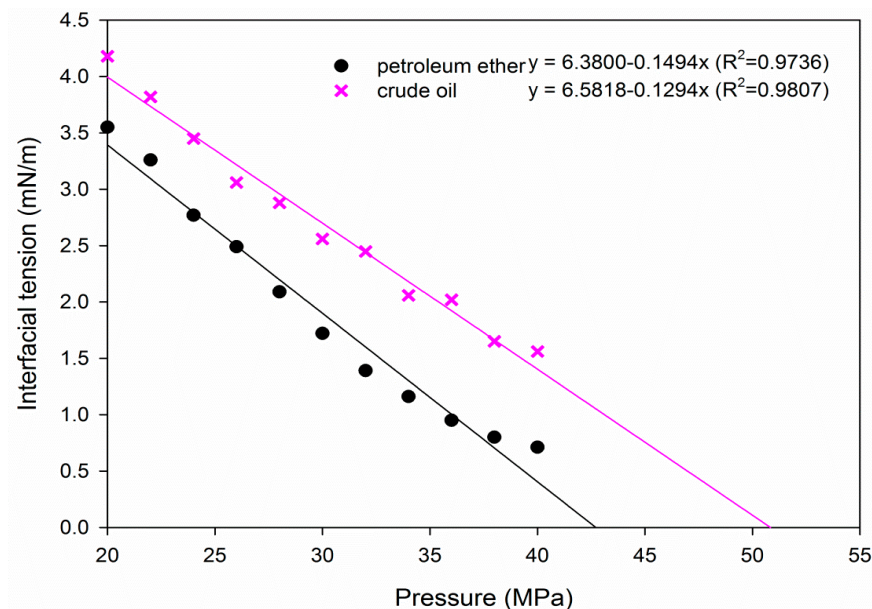


Figure 4. Changes of CO₂–oil interfacial tensions with pressures for diluted crude oil with petroleum ether and undiluted crude oil.

2.3. Discussions

The hydrocarbon agent reduced the IFT between crude oil and CO₂ and further decreased the MMP. This was related with the change of crude oil property caused by the enhanced extraction of light components from crude oil with the hydrocarbon agent.

The critical point of CO₂ is at 31.2 °C and 7.38 MPa. At most reservoir conditions, the CO₂ injected into the reservoir is in a supercritical state. Theoretically, supercritical CO₂ can enter any void space larger than its molecules. CO₂ is highly sensitive to changes in pressure and temperature when the system is around its critical point, and its physical properties—including density and viscosity—change rapidly [48].

In the supercritical system, when CO₂ makes contact with a raw material such as a solvent, some light components in the raw material will be vaporized by the solvent. After that, the solute dissolved in supercritical fluid can be precipitated with changing temperature and pressure. Then, the component extraction can be realized.

The component contents of the crude oil mixed with petroleum ether and extracted by CO₂ at 30 MPa of pressure were measured with a total hydrocarbon gas chromatograph, and the statistical results are shown in Figure 5. The mole fraction of C5-C12 in crude oil under atmospheric pressure was higher than that extracted by CO₂ under high pressure. For the crude oil sample, which was mixed with petroleum ether and extracted by CO₂, the mole fractions of C5-C12 in it were about 6% lower than that without petroleum ether under the same pressure condition and CO₂ extraction. This indicates that the hydrocarbon agent (petroleum ether) could promote CO₂ to extract light hydrocarbon components from crude oil. The mole fractions of the middle distillate (C13-C18) for three scenarios were close. However, the mole fractions of the residual hydrocarbons (C19-C35+) were significantly different. Among them, the mole fraction of C19-C35+ of petroleum ether under 30 MPa of pressure was up to 52.1%, which was approximately 15.6% higher than that of crude oil under atmospheric pressure conditions.

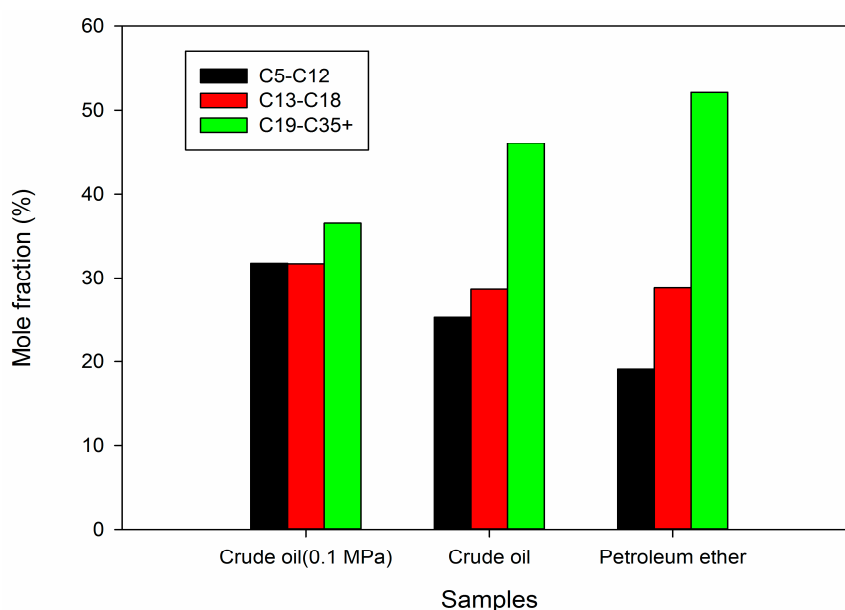


Figure 5. Mole fractions of hydrocarbons after the crude oil diluted with petroleum ether and undiluted crude oil at the pressure of 30 MPa.

The hydrocarbon agent improved the ability of CO₂ to extract light components from crude oil. Under reservoir temperatures and pressure conditions and without a hydrocarbon agent, CO₂ would not further extract hydrocarbons; CO₂ and crude oil achieve an equilibrium state. In terms of the carbon atom number of the selected hydrocarbon agents, they were the light components in the crude oil. The addition of such hydrocarbon agents in crude oil was equivalent to increasing the mole fraction of a light hydrocarbon component. Under the reservoir condition, the CO₂-oil miscibility development was a multi-contact process in which CO₂ vaporized the light components in the leading front and condensed at the trailing end. If the reservoir oil did not have sufficient light components, the vaporization process would fail, as would the later condensation process. When a light component such as petroleum ether was added, it enriched the oil in places, which facilitated the miscibility development. Since the added light components had high affinities to CO₂, the IFT between the CO₂ and the enriched oil decreased. Usually, the stronger the affinity between CO₂ and oil is, the less the IFT between CO₂ and oil will be. As the data show in Table 2, the IFT between CO₂ and crude oil with a hydrocarbon agent (petroleum ether) was lower than that without it at the same pressure. The experimental and the theoretical results verify that reducing the IFT directly led to the decrease of CO₂-oil MMP.

Additionally, CO₂ dissolved in crude oil could not only cause the crude oil swelling and increase the reservoir pressure, but it could also reduce viscosity and IFT, which is beneficial for improving oil recovery [49–51]. A high solubility of CO₂ in crude oil was beneficial in decreasing the CO₂-oil

MMP. The solubility of CO₂ in crude oil mixed with different hydrocarbon agents was measured, and the results are shown in Figure 6. The solubility of CO₂ in crude oil increased with the increase of pressure in isothermal conditions. There were no significant changes between the crude oil samples with and without hydrocarbon agents. Therefore, it can be concluded that the hydrocarbon agent had no impact on the solubility of CO₂ in crude oil, and it only affected the extracting capacity of CO₂ on intermediate hydrocarbons.

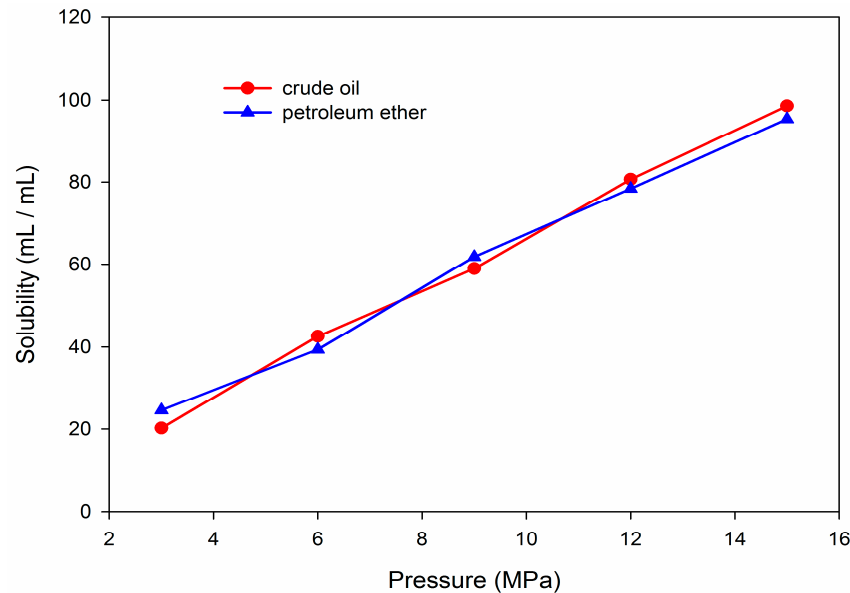


Figure 6. Solubility of CO₂ in the diluted crude oil with petroleum ether and undiluted crude oil under different pressures.

3. Screening and Evaluation of Hydrocarbon Agents

3.1. Influence of Hydrocarbon Agents on CO₂–Oil IFT and MMP

In order to select a suitable hydrocarbon agent for reservoir crude oil in the H Block, four types of hydrocarbon agents (including alkanes, alcohols, oil-soluble surfactants, and petroleum ethers) were tested and evaluated. The IFTs for different hydrocarbon agents were measured under the temperature of 109 °C and a mass concentration of hydrocarbon agents of 0.5%.

3.1.1. Alkane Type

According to the previous research experiments on CO₂ flooding in the Cooper Basin, South Australia by Bon and Sarma, C₅+ can significantly reduce CO₂–oil IFT [52]. Therefore, we selected n-pentane, n-hexane, and iso-octane for evaluation, and the results are shown in Figure 7. Figure 7 shows that the CO₂–oil IFT decreased with the increasing pressure. For the same alkane, the difference of CO₂–oil IFT between 20 MPa and 40 MPa was about 3 mN/m. Under the same pressure condition, the CO₂–oil IFTs with different alkanes were lower than those without the hydrocarbon agent. The CO₂–oil IFT without a hydrocarbon agent was 1.563 mN/m at 40 MPa, which was about 0.5 mN/m higher than that with different alkanes. Therefore, alkanes could reduce the CO₂–oil IFT. Using the linear extrapolation method, the CO₂–oil MMPs for n-pentane, n-heptane, and iso-octane were 45.93 MPa, 46.10 MPa, and 46.27 MPa, respectively. The addition of alkane hydrocarbon agents could reduce the CO₂–oil MMP. With the increase of carbon numbers in alkanes, the ability to reduce CO₂–oil MMP decreased [53]. Compared with the crude oil without a hydrocarbon agent, the IFT of CO₂–oil with n-pentane was reduced by 4.93 MPa or 9.69%.

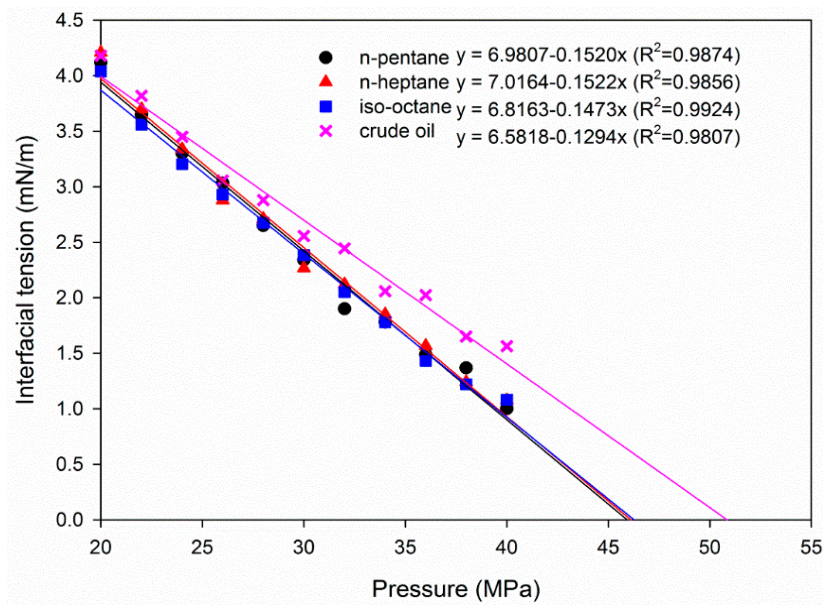


Figure 7. Changes of CO₂–oil IFTs with pressures for the crude oil diluted with different alkanes.

3.1.2. Alcohol Type

N-butyl alcohol and n-amyl alcohol were used to evaluate their capacities on reducing CO₂–oil MMP, and the results are presented in Figure 8. For the same alcohol, the difference of CO₂–oil IFT between 20 MPa and 40 MPa was about 2.8 mN/m. However, the difference of CO₂–oil IFT between n-butyl alcohol and n-amyl alcohol was small under the same pressure. The CO₂–oil IFT with n-butyl alcohol was 1.11 mN/m at 40 MPa, which was about 0.453 mN/m lower than that without a hydrocarbon agent. The extrapolated CO₂–oil MMPs for n-butyl alcohol and n-amyl alcohol were 46.58 MPa and 46.76 MPa, respectively, which indicates that they had similar abilities to reduce the CO₂–oil MMP.

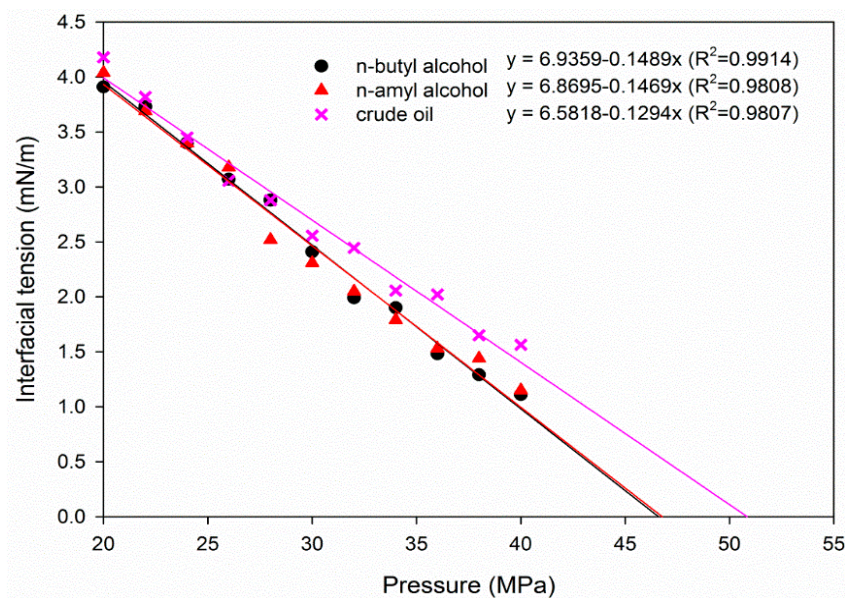


Figure 8. Changes of CO₂–oil IFTs with pressures for the crude oil diluted with different alcohols.

3.1.3. Oil-Soluble Surfactant Type

Alkylphenol polyoxyethylene ether [APO, C₈H₁₇-C₆H₄-O-(CH₂CH₂O)₁₀-H], fatty alcohol polyoxyethylene ether [AEO, C₁₂-O-(CH₂CH₂O)₁₅-H], and ethylene glycol butyl ether were added in

the crude oil to determine their abilities in reducing CO₂–oil IFTs. The changes of the CO₂–oil IFTs with pressure after mixing with different oil-soluble surfactants are shown in Figure 9. For the same oil-soluble surfactant, the difference of CO₂–oil IFTs between 20 MPa and 40 MPa was about 2.6 mN/m. The CO₂–oil IFT with ethylene glycol butyl ether was smaller than that with APO and AEO at the same pressure. However, there was no significant IFT difference between crude oil without a hydrocarbon agent and that with APO and AEO, which indicates that APO and AEO had little effect on reducing CO₂–oil MMP. The extrapolated CO₂–oil MMPs for ethylene glycol butyl ether, APO, and AEO were 46.65 MPa, 49.29 MPa, and 49.05 MPa, respectively. Among these oil-soluble surfactants, the ethylene glycol butyl ether reduced the CO₂–oil MMP by a maximum of 4.21 MPa or 8.28%.

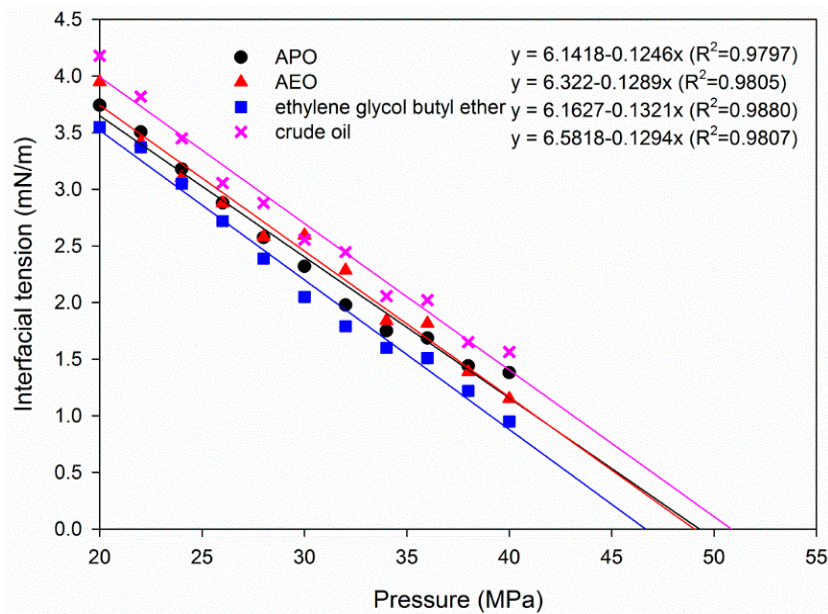


Figure 9. Changes of CO₂–oil IFTs with pressures for the crude oil diluted with different oil-soluble surfactants.

3.1.4. Petroleum Ether Type

Petroleum ether is a colorless liquid, and its main compositions are pentane and hexane. The boiling points of different petroleum ethers can be 30–60 °C, 60–90 °C, or 90–120 °C. Their effects on CO₂–oil IFT under different pressures are shown in Figure 10. Under the same pressure condition, the lowest CO₂–oil IFT was petroleum ether with a boiling range of 30–60 °C, and the highest was that of 90–120 °C. The deduced CO₂–oil MMPs for boiling ranges of 30–60 °C, 60–90 °C, and 90–120 °C were 44.67 MPa, 45.52 MPa, and 45.84 MPa, respectively. With the increasing boiling range of petroleum ether, the reduction on CO₂–oil MMP gradually decreased. Among these petroleum ethers, the boiling range of 30–60 °C was superior to others, which resulted in a pressure reduction by 6.19 MPa or 12.17%. This indicates that the petroleum ether with a lower boiling temperature had a higher affinity with CO₂ than others. Therefore, the effect of reducing the CO₂–oil MMP was also more remarkable.

Based on the above measurements, the best hydrocarbon agent for reservoir oil in the H Block to achieve MMP is the petroleum ether in the boiling range of 30–60 °C.

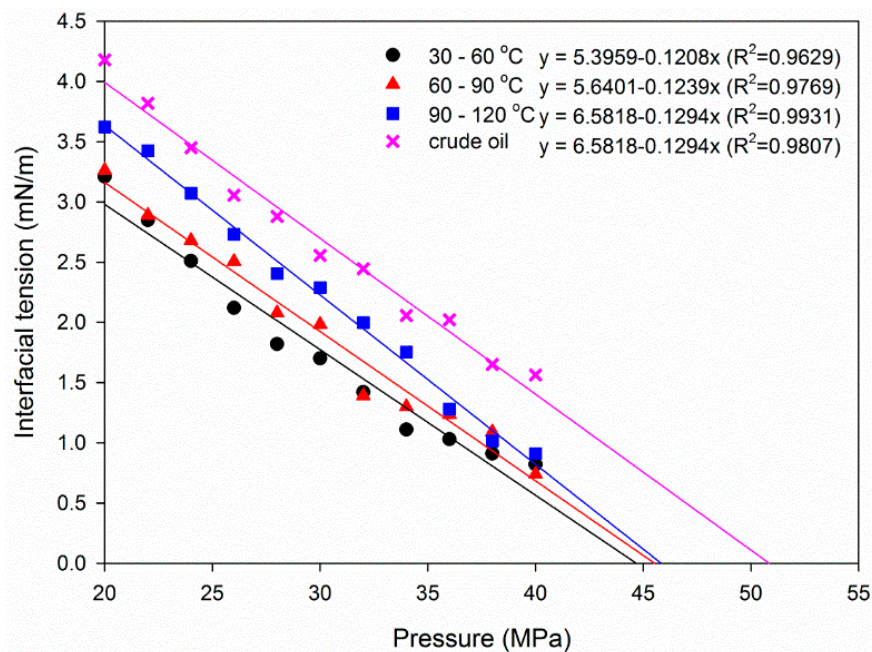


Figure 10. Changes of CO₂–oil IFTs with pressures for the crude oil diluted with different petroleum ethers.

3.2. Influence of Mass Concentration of Petroleum Ether on CO₂–Oil Interfacial Tension and Miscibility Pressure

The mass concentration of petroleum ether not only affects CO₂–oil interfacial tension and miscibility pressure; it also affects the operation cost. To determine the optimal mass concentration for petroleum ether (the boiling range of 30–60 °C in this study), petroleum ether with different mass concentrations (0.1%, 0.3%, 0.5%, 0.7%, and 0.9%) was mixed with crude oil to study the effect on CO₂–oil interfacial tension and miscibility pressure. The results are shown in Figures 11 and 12.

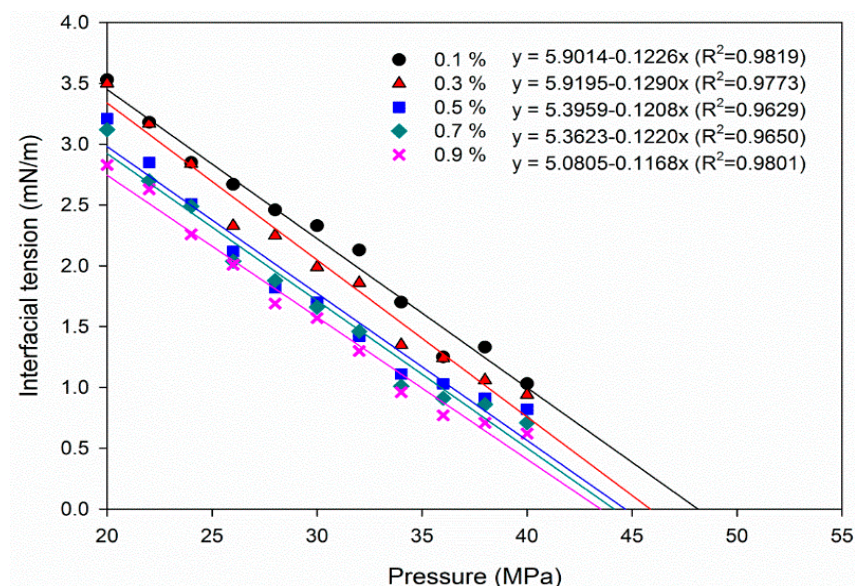


Figure 11. Changes of CO₂–oil IFTs with pressures for the crude oil diluted with different mass concentrations of petroleum ether in the boiling range of 30–60 °C.

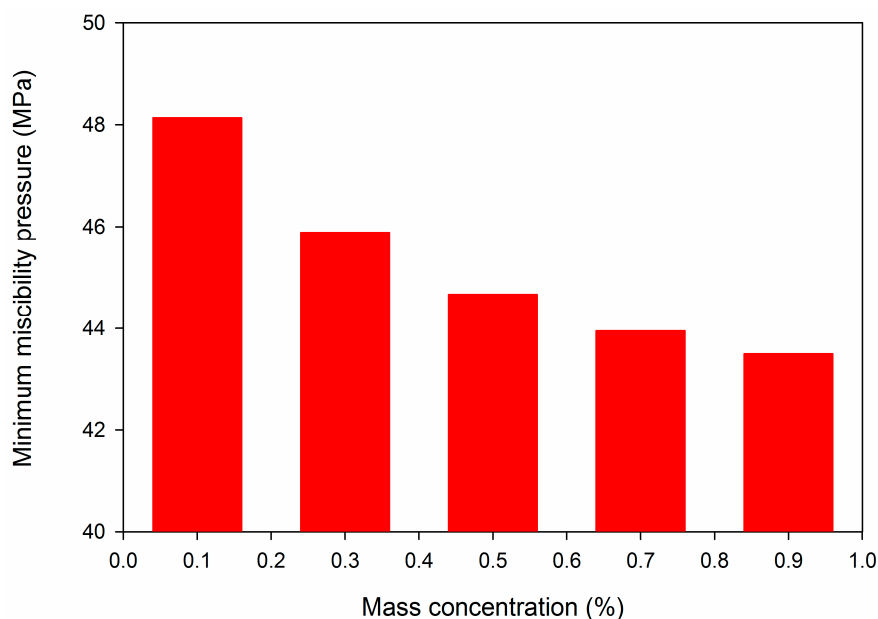


Figure 12. CO₂-oil MMPs for the crude oil diluted with different mass concentrations of petroleum ether in the boiling range of 30–60 °C.

We can see that both the CO₂-oil IFT and MMP decreased with the increase of mass concentration of petroleum ether. When the mass concentration of petroleum ether was between 0.1% and 0.5%, the CO₂-oil MMP was sensitive to the mass concentration. The CO₂-oil MMPs with mass concentrations of 0.1% and 0.3% were about 3.47 MPa and 1.22 MPa higher than those with a mass concentration of 0.5%, respectively. The sensitivity of CO₂-oil MMP to the mass concentration of petroleum ether decreased when the mass concentration was above 0.5%. The CO₂-oil MMPs with a mass concentration of 0.5% were 0.72 MPa and 1.17 MPa higher than those with mass concentrations of 0.7% and 0.9%, respectively. Given the additional cost of petroleum ether and the potential of reducing CO₂-oil MMP, the mass concentration of 0.5% is recommended for reservoir crude oil in the H Block.

3.3. Influence of Hydrocarbon Agents on Crude Oil Viscosity

Different hydrocarbon agents with a mass concentration of 0.5% were mixed with crude oil, and their viscosities under different temperatures were measured (Table 3). The oil viscosity had a strong sensitivity to temperature within the scope of 40–50 °C, and it declined slowly when the temperature exceeded 50 °C.

Table 3. Oil viscosities for the diluted crude oil with different hydrocarbon agents and undiluted crude oil under different temperatures.

Temperature (°C)	Viscosity (mPa·s)				
	Ethylene Glycol Butyl Ether	N-butyl Alcohol	Petroleum Ether	N-pentane	Crude Oil
40	88.5	58.5	70.5	49.8	76.4
50	17.6	14.2	15.1	15.2	17.4
60	10.5	10.2	10.8	9.8	12.8
70	7.4	7.7	8.7	8.6	9.8

The effects of mass concentrations of petroleum ether with a boiling range of 30–60 °C on crude oil viscosity were also measured at the temperature of 70 °C. The results are given in Table 4. With the increase of mass concentration of petroleum ether, the crude oil viscosity decreased. The oil viscosity difference between mass concentrations of 0.5% and 0.9% was 0.8 mPa·s. This indicates that the effect

of excessive increase of the mass concentration of petroleum ether on crude oil viscosity was not very prominent. Considering the economic factor, the recommended mass concentration of petroleum ether is 0.5%.

Table 4. Oil viscosities for the crude oil diluted with different mass concentrations of petroleum ether at the temperature of 70 °C.

Mass concentration of petroleum ether (%)	0.1	0.3	0.5	0.7	0.9
Viscosity (mPa·s)	10.5	9.5	8.7	8.2	7.9

3.4. Influence of Hydrocarbon Agents on Injectivity

As the hydrocarbon agents are usually injected as slugs prior to CO₂ flooding, we studied four types of hydrocarbon agents (including ethylene glycol monobutyl ether, n-butyl alcohol, petroleum ether in the boiling range of 30–60 °C, and n-pentane) with a mass concentration of 0.5% to evaluate their injectivities. Four synthetic cores with a length of 60 mm, a diameter of 25 mm, a porosity of $15.4 \pm 0.2\%$, and a gas permeability of $10 \pm 0.2 \times 10^{-3} \mu\text{m}^2$ were used to conduct injection tests. The measured pressure differences and the calculated pressure gradients at different injection rates are shown in Table 5. According to the method of calculating pseudo-starting pressure from a typical non-Darcy flow curve [54], the linear extrapolated minimum starting pressure gradients for petroleum ether in the boiling range of 30–60 °C, n-pentane, n-butyl alcohol, and ethylene glycol monobutyl ether were 0.0411 MPa/cm, 0.0436 MPa/cm, 0.0662 MPa/cm, and 0.1295 MPa/cm, respectively. The results show that petroleum ether in the boiling range of 30–60 °C is easiest to inject into the reservoir.

Table 5. Pressure gradient of different hydrocarbon agents at the temperature of 70 °C.

Q (mL/min)	Pressure Gradient (MPa/cm)			
	Ethylene Glycol Monobutyl Ether	N-butyl Alcohol	Petroleum Ether (30–60 °C)	N-pentane
0.05	0.187	0.125	0.086	0.087
0.10	0.290	0.191	0.155	0.151
0.20	0.412	0.289	0.242	0.252
0.30	0.554	0.427	0.351	0.343

4. Conclusions

The mechanism of using a hydrocarbon agent to reduce CO₂–oil MMP was studied through IFT measurement and oil compositional analysis, and the optimal hydrocarbon agent and its mass concentration suitable for reservoir crude oil in the H Block were screened. The influence of hydrocarbon agents on crude oil viscosity and its injection capacity were also evaluated. From these studies, the following conclusions can be drawn.

- (1) Adding hydrocarbon agents into crude oil can reduce the CO₂–oil IFT and lower the MMP.
- (2) Alkanes, alcohols, oil-soluble surfactants, and petroleum ethers tested in this study are all beneficial to reducing CO₂–oil interfacial tension and CO₂–oil minimum miscibility pressure for the reservoir crude oil in the H Block. Among these, the petroleum ether in the boiling range of 30–60 °C was selected, since it yielded the minimum MMP.
- (3) The mass concentration of hydrocarbon agents has a remarkable effect on CO₂–oil minimum miscibility pressure and crude oil viscosity. The experiments on CO₂–oil interfacial tension and crude oil viscosity under different mass concentrations suggest that the petroleum ether in the boiling range of 30–60 °C with a mass concentration of 0.5% would be the best hydrocarbon agent for implementing CO₂ miscible flooding in the H Block.

Author Contributions: Conceptualization, Z.L. and J.L.; methodology, Z.L. and J.L.; validation, L.S., Z.L. and J.L.; investigation, L.S. and Z.L.; writing—original draft preparation, J.L. and L.S.; writing—review and editing, J.L. and X.W.; visualization, J.L. and L.S.; supervision, J.L. and Z.L.

Funding: This research was funded by “the National Natural Science Foundation of China, grant number 51674278” and “the Changjiang Scholars and the Innovative Research Team in University, grant number IRT1294”.

Conflicts of Interest: The authors declare no conflict of interest.

References

1. Verma, M.K. *Fundamentals of Carbon Dioxide-Enhanced Oil Recovery (CO₂-EOR): A Supporting Document of the Assessment Methodology for Hydrocarbon Recovery using CO₂-EOR Associated with Carbon Sequestration*; US Department of the Interior: Washington, DC, USA, 2015.
2. NETL US Department of Energy. Enhanced Oil Recovery. Available online: <https://www.energy.gov/fe/science-innovation/oil-gas-research/enhanced--oil-recovery> (accessed on 9 April 2019).
3. Glaso, O. Generalized minimum miscibility pressure correlation (includes associated papers 15845 and 16287). *Soc. Pet. Eng. J.* **1985**, *25*, 927–934. [[CrossRef](#)]
4. Orr, F., Jr.; Yu, A.; Lien, C. Phase behavior of CO₂ and crude oil in low-temperature reservoirs. *Soc. Pet. Eng. J.* **1981**, *21*, 480–492. [[CrossRef](#)]
5. National Energy Technology Laboratory (NETL). *Recovery, Carbon Dioxide Enhanced Oil, Untapped Domestic Energy Supply and Long Term Carbon Storage Solution*; National Energy Technology Laboratory (NETL), US Department of Energy: Washington, DC, USA, 2010.
6. Li, S.L.; Guo, P.; Dai, L.; Sun, L. Strengthen gas injection for enhanced oil recovery. *J. Southwest Pet. Inst.* **2000**, *22*, 41–45.
7. Shen, P.P.; Jiang, H.Y.; Che, Y.W.; Li, Y.T.; Liu, J.S. EOR study of CO₂ injection. *SPEC Oil Gas Reserv.* **2007**, *14*, 1–4.
8. Li, B.F.; Ye, J.Q.; Li, Z.M.; Ji, Y.M.; Liu, W. Phase interaction of CO₂–oil–water system and its effect on interfacial tension at high temperature and high pressure. *Acta Pet. Sin.* **2016**, *37*, 1265–1272.
9. Han, H.S.; Li, S.; Chen, X.L.; Qin, J.S.; Zeng, B.Q. Main control factors of carbon dioxide on swelling effect of crude hydrocarbon components. *Acta Pet. Sin.* **2016**, *37*, 392–398.
10. Tang, M.M.; Zhao, H.Y.; Ma, H.F.; Lu, S.F.; Chen, Y.M. Study on CO₂ huff-n-puff of horizontal wells in continental tight oil reservoirs. *Fuel* **2017**, *188*, 140–154. [[CrossRef](#)]
11. Peng, X.Y.; Wang, Y.Y.; Diao, Y.Q.; Zhang, L.; Yazid, I.M.; Ren, S.R. Experimental investigation on the operation parameters of carbon dioxide huff-n-puff process in ultra low permeability oil reservoirs. *J. Pet. Sci. Eng.* **2019**, *174*, 903–912. [[CrossRef](#)]
12. Li, L.; Zhang, Y.; Sheng, J.J. Effect of the Injection Pressure on Enhancing Oil Recovery in Shale Cores during the CO₂ Huff-n-Puff Process When It Is above and below the Minimum Miscibility Pressure. *Energy Fuels* **2017**, *31*, 3856–3867. [[CrossRef](#)]
13. Zuloaga, P.; Yu, W.; Miao, J.J.; Sepehrnoori, K. Performance evaluation of CO₂ Huff-n-Puff and continuous CO₂ injection in tight oil reservoirs. *Energy* **2017**, *134*, 181–192. [[CrossRef](#)]
14. Fox, M.J.; Simlote, V.N.; Beaty, W.G. *Evaluation Of CO₂ Flood Performance*; Springer: Garvin County, NE, USA, 1984.
15. Martin, F.D. Carbon dioxide flooding. *J. Can. Pet. Technol.* **1992**, *44*, 396–400. [[CrossRef](#)]
16. Langston, M.V.; Hoadley, S.F.; Young, D.N. Definitive CO₂ Flooding Response in the SACROC Unit. In Proceedings of the SPE Enhanced Oil Recovery Symposium, Tulsa, OA, USA, 16–21 April 1988.
17. Koottungal, L. 2004 worldwide EOR survey. *Oil Gas J.* **2004**, *102*, 53–65.
18. Koottungal, L. 2006 worldwide EOR survey. *Oil Gas J.* **2006**, *104*, 45–57.
19. Koottungal, L. 2008 worldwide EOR survey. *Oil Gas J.* **2008**, *106*, 47–59.
20. Koottungal, L. 2010 worldwide EOR survey. *Oil Gas J.* **2010**, *108*, 41–53.
21. Koottungal, L. 2012 worldwide EOR survey. *Oil Gas J.* **2012**, *110*, 57–69.
22. Koottungal, L. 2014 worldwide EOR survey. *Oil Gas J.* **2014**, *112*, 79–91.
23. Welkenhuysen, K.; Meyvis, B.; Piessens, K. A Profitability Study of CO₂-EOR and Subsequent CO₂ Storage in the North Sea under Low Oil Market Prices. *Energy Procedia* **2017**, *114*, 7060–7069. [[CrossRef](#)]

24. Welkenhuysen, K.; Meyvis, B.; Swennen, R.; Piessens, K. Economic threshold of CO₂-EOR and CO₂ storage in the North Sea: A case study of the Claymore, Scott and Buzzard oil fields. *Int. J. Greenh. Gas Control* **2018**, *78*, 271–285. [[CrossRef](#)]
25. Cavanagh, A.; Ringrose, P. Improving Oil Recovery and Enabling CCS: A Comparison of Offshore Gas-recycling in Europe to CCUS in North America. *Energy Procedia* **2014**, *63*, 7677–7684. [[CrossRef](#)]
26. Fleten, S.-E.; Lien, K.; Ljønes, K.; Pagès-Bernaus, A.; Aaberg, M. Value chains for carbon storage and enhanced oil recovery: Optimal investment under uncertainty. *Energy Syst.* **2010**, *1*, 457–470. [[CrossRef](#)]
27. Guo, D.B.; Fang, Q.; Nie, F.J. Study on EOR of injection CO₂ for waterflooding abandoned reservoir. *Fault Block Oil Gas Field* **2012**, *19*, 187–190.
28. Zhang, J.; Zhou, Z.W.; Wang, W.S.; Tao, L.B. EOR field test of gas-water alternative injection in Pubei oilfield. *Pet. Explor. Dev.* **2004**, *31*, 85–87.
29. Hao, Y.M.; Chen, Y.M.; Ying, H.L. Determination and prediction of minimum miscibility pressure in CO₂ flooding. *Pet. Geol. Recovery Effic.* **2005**, *12*, 64–66.
30. Ju, B.S.; Qin, J.S.; Li, Z.P.; Chen, X. A prediction model for the minimum miscibility pressure of the CO₂-crude oil system. *Acta Pet. Sin.* **2012**, *33*, 274–277.
31. Bon, J.; Sarma, H.K.; Theophilos, A.M. An Investigation of Minimum Miscibility Pressure for CO₂—Rich Injection Gases with Pentanes-Plus Fraction. In Proceedings of the SPE International Improved Oil Recovery Conference in Asia Pacific, Kuala Lumpur, Malaysia, 5–6 December 2005.
32. Liu, Y.; Jiang, L.L.; Song, Y.C.; Zhao, Y.C.; Zhang, Y.; Wang, D.Y. Estimation of minimum miscibility pressure (MMP) of CO₂ and liquid n-alkane systems using an improved MRI technique. *Magn. Reson. Imaging* **2016**, *34*, 97–104. [[CrossRef](#)]
33. Guo, P.; Li, M. A study on the miscible conditions of CO₂ injection in low-permeability sandstone reservoirs. *Oil Gas Geol.* **2007**, *28*, 687–690.
34. Yao, Y.D.; Wang, Z.J.; Li, G.Z.; Wu, H.; Wang, J.N. Potential of carbon dioxide miscible injections into the H-26 reservoir. *J. Nat. Gas Sci. Eng.* **2016**, *34*, 1085–1095. [[CrossRef](#)]
35. Kaydani, H.; Najafzadeh, M.; Hajizadeh, A. A new correlation for calculating carbon dioxide minimum miscibility pressure based on multi-gene genetic programming. *J. Nat. Gas Sci. Eng.* **2014**, *21*, 625–630. [[CrossRef](#)]
36. Chen, G.Y.; Gao, H.X.; Fu, K.Y.; Zhang, H.Y.; Liang, Z.W.; Tontiwachwuthikul, P. An improved correlation to determine minimum miscibility pressure of CO₂–oil system. *Green Energy Environ.* **2018**. [[CrossRef](#)]
37. Christiansen, R.L.; Haines, H.K. Rapid Measurement of Minimum Miscibility Pressure With the Rising-Bubble Apparatus. *SPE Reserv. Eng.* **1987**, *2*, 523–527. [[CrossRef](#)]
38. Zhou, D.; Orr, F.M., Jr. An Analysis of Rising Bubble Experiments to Determine Minimum Miscibility Pressures. *SPE J.* **1988**, *3*, 19–25. [[CrossRef](#)]
39. Nobakht, M.; Moghadam, S.e.; Gu, Y.A. Determination of CO₂ Minimum Miscibility Pressure from Measured and Predicted Equilibrium Interfacial Tensions. *Ind. Eng. Chem. Res.* **2008**, *47*, 8918–8925. [[CrossRef](#)]
40. Rao, D.N.; Lee, J.I. Application of the new vanishing interfacial tension technique to evaluate miscibility conditions for the Terra Nova Offshore Project. *J. Pet. Sci. Eng.* **2002**, *35*, 247–262. [[CrossRef](#)]
41. Wu, R.S.; Batycky, J.P. Evaluation Of Miscibility From Slim Tube Tests. *J. Can. Pet. Technol.* **1990**, *29*, 9. [[CrossRef](#)]
42. Czarnota, R.; Janiga, D.; Stopa, J.; Wojnarowski, P. Determination of minimum miscibility pressure for CO₂ and oil system using acoustically monitored separator. *J. CO₂ Util.* **2017**, *17*, 32–36. [[CrossRef](#)]
43. Mihcakan, M. Minimum Miscibility Pressure, Rising Bubble Apparatus, and Phase Behavior. In Proceedings of the SPE/DOE Improved Oil Recovery Symposium, Tulsa, OA, USA, 17–20 April 1994.
44. Rao, D.N. A new technique of vanishing interfacial tension for miscibility determination. *Fluid Phase Equilib.* **1997**, *139*, 311–324. [[CrossRef](#)]
45. Andreas, J.H.; Hauser, E.A.; Tucker, W.B. Boundary tension by pendant drops. *J. Phys. Chem.* **1938**, *42*, 1001–1019. [[CrossRef](#)]
46. Peng, B.Z.; Luo, H.; Chen, G.J.; Sun, C.Y. Determination of the minimum miscibility pressure of CO₂ and crude oil system by vanishing interfacial tension method. *Acta Pet. Sin.* **2007**, *28*, 93–95.
47. Luo, K.; Chen, G. Application of the Gas-Oil Interfacial Tension to Determine Minimum Miscibility Pressure. In Proceedings of the Canadian International Petroleum Conference, Calgary, AL, Canada, 17–19 June 2001.
48. Wang, H.Z.; Shen, Z.H.; Li, G.S. Feasibility analysis on shale gas exploitation with supercritical CO₂. *Pet. Drill. Tech.* **2011**, *39*, 30–34.

49. Czarnota, R.; Janiga, D.; Stopa, J.; Wojnarowski, P. Acoustic investigation of CO₂ mass transfer into oil phase for vapor extraction process under reservoir conditions. *Int. J. Heat Mass Transf.* **2018**, *127*, 430–437. [[CrossRef](#)]
50. Rudyk, S.; Spirov, P.; Tyrovolas, A. Effect of temperature on crude oil extraction by SC-CO₂ at 40–70 °C and 40–60 MPa. *J. CO₂ Util.* **2018**, *24*, 471–478. [[CrossRef](#)]
51. Li, H.Z.; Zheng, S.X.; Yang, D.Y. Enhanced Swelling Effect and Viscosity Reduction of Solvents-CO₂-Heavy Oil Systems. In Proceedings of the SPE Heavy Oil Conference and Exhibition, Kuwait City, Kuwait, 12–14 December 2011.
52. Bon, J.; Sarma, H.K. A Technical Evaluation of a CO₂ Flood for EOR Benefits in the Cooper Basin, South Australia. In Proceedings of the SPE Asia Pacific Oil and Gas Conference and Exhibition, Perth, Australia, 18–20 October 2004.
53. Deng, R.J.; Qi, G.X.; Tan, X.; Li, P.C. Influence of hydrocarbon components on the minimum miscibility pressure of CO₂ flooding. *Chem. Eng. Oil Gas* **2018**, *47*, 59–63. [[CrossRef](#)]
54. Shi, J.P.; Shao, X.Q.; Ma, J.H.; Zhang, X.L.; Yang, X.D.; Cao, W.Z. Application of experimentally determined minimum starting pressure gradient of low permeability reservoir. *Pet. Geol. Oilfield Dev. Daqing* **2010**, *29*, 81–83. [[CrossRef](#)]



© 2019 by the authors. Licensee MDPI, Basel, Switzerland. This article is an open access article distributed under the terms and conditions of the Creative Commons Attribution (CC BY) license (<http://creativecommons.org/licenses/by/4.0/>).